Interactions of Alamethicin with Model Cell Membranes Investigated Using Sum Frequency Generation Vibrational Spectroscopy in Real Time in Situ

Shuji Ye,[†,‡] Khoi Tan Nguyen,[†] and Zhan Chen*[,†]

Department of Chemistry, University of Michigan, Ann Arbor, Michigan 48109, and Hefei National Laboratory for Physical Sciences at Microscale, University of Science and Technology of China, Hefei, Anhui, P. R. China 230026

Received: November 24, 2009; Revised Manuscript Received: January 24, 2010

Structures of membrane-associated peptides and molecular interactions between peptides and cell membrane bilayers govern biological functions of these peptides. Sum frequency generation (SFG) vibrational spectroscopy has been demonstrated to be a powerful technique to study such structures and interactions at the molecular level. In this research, SFG has been applied, supplemented by attenuated total reflectance Fourier transform infrared spectroscopy (ATR-FTIR), to characterize the interactions between alamethicin (a model for larger channel proteins) and different lipid bilayers in the absence of membrane potential. The orientation of alamethicin in lipid bilayers has been determined using SFG amide I spectra detected with different polarization combinations. It was found that alamethicin adopts a mixed α-helical and 3_{10}-helical structure in fluid-phase lipid bilayers. The helix (mainly α-helix) at the N-terminus tilts at about 63° versus the surface normal in a fluid-phase 1,2-dimyristoyl-*d*54-*sn*-glycero-3-phosphocholine-1,1,2,2-*d*4-*N*,*N*,*N*-trimethyl-*d*9 (*d*-DMPC)/1,2-dimyristoyl-*sn*-glycero-3-phosphocholine (DMPC) bilayer. The 3_{10}-helix at the C-terminus (beyond the Pro14 residue) tilts at about 43° versus the surface normal. This is the first time to apply SFG to study a 3_{10}-helix experimentally. When interacting with a gel-phase lipid bilayer, alamethicin lies down on the gel-phase bilayer surface or aggregates or both, which does not have significant insertion into the lipid bilayer.

1. Introduction

Ion channels represent an important class of transmembrane proteins that regulate ionic permeability in cell membranes. They are key elements in signaling and sensing pathways, as well as connecting the inside of the cell to its outside in a selective fashion.[1] They play crucial roles in normal and pathophysiological functions of cells. Defective ion channels can lead to many diseases, such as cystic fibrosis, cardiac arrhythmias, and Parkinson's disease.[2−9] Investigations on structures of these membrane proteins will aid in the understanding of disease mechanisms and provide important clues to cure such diseases.

Alamethicin is a 20-residue hydrophobic antibiotic peptide extracted from the fungus *Trichoderma viride* that can form voltage-gated ion channels in membranes.[10−23] It has been used frequently as a model for larger channel proteins.[10−18] In addition to the regular amino acids, the peptide contains eight aminoisobutyric acid units. The molecular structure and conformational features of alamethicin have been studied extensively.[10−27] The crystal structure of alamethicin crystallized from methanol determined by X-ray diffraction is predominantly helical, with an N-terminal α-helix and a C-terminal domain beyond the Pro14 residue that contains a 3_{10}-helical element.[24] Pro14 residue acts as a bend in the helix, and the bend angle between the two helical axes is about 20−35°.[24]

Extensive research has been performed to examine the mechanisms of alamethicin's action on cell membranes.[10−23] It is currently believed that alamethicin interacts with cell membranes through the barrel-stave mode, with the resulting conducting pores in the membrane formed by parallel bundles of 3−12 helical alamethicin monomers surrounding a central, water-filled pore.[12,13,22−24,28−30] However, further details of the mechanism of alamethicin channel formation at the molecular level are still far from completion.[31,32] In addition, contradictory orientations of alamethicin in the cell membranes in the absence of membrane potential have been reported. Alamethicin has been suggested to adopt a transmembrane orientation,[25−27,33−37] lie down on the membrane surface,[38−40] or both (depending on the experimental conditions).[41,42] A continuous distribution of orientations has also been proposed.[43]

A detailed characterization of interactions between alamethicin and model membranes without a transmembrane potential is a fundamental step in the understanding of the operational mechanisms of ion channels. However, as mentioned above, different results have been reported in the literature. In this research, we applied sum frequency generation (SFG) vibrational spectroscopy supplemented by attenuated total reflectance Fourier transform infrared spectroscopy (ATR-FTIR) to investigate the interactions between alamethicin and different lipid bilayers. SFG is a nonlinear optical laser technique that provides vibrational spectra of surfaces and interfaces.[44−66] It has several advantages over other analytical techniques: it is intrinsically surface-sensitive, requires small amounts of samples, and can probe surfaces and interfaces in situ in real-time. As a polarized vibrational spectroscopy, SFG permits the identification of interfacial molecular species (or chemical groups) and also provides information about the interfacial structure, such as the orientation and the orientation distribution of functional groups on a surface or at an interface.[44−55] SFG has been applied to study the structure and orientation of various biomolecules (including peptides and proteins) in interfacial environments.[56−64] Here, we deduced the orientation of alamethicin by analyzing the polarized SFG amide I signals without the presence of membrane potential, which will serve as a basis for future SFG

* To whom correspondence should be addressed. Fax: 734-647-4865. E-mail: zhanc@umich.edu.
[†] University of Michigan.
[‡] University of Science and Technology of China.

10.1021/jp911174d
Published on Web 02/17/2010

TABLE 1: Lipids Studied in This Paper

abbrev	full name
POPC	1-palmitoyl-2-oleoyl-*sn*-glycero-3-phosphocholine
POPG	1-palmitoyl-2-oleoyl-*sn*-glycero-3-[phospho-*rac*-(1-glycerol)] (sodium salt)
DMPC	1,2-dimyristoyl-*sn*-glycero-3-phosphocholine
d-DMPC	1,2-dimyristoyl-*d*54-*sn*-glycero-3-phosphocholine-1,1,2,2-*d*4-*N*,*N*,*N*-trimethyl-*d*9
DPPC	1,2-dipalmitoyl-*sn*-glycero-3-phosphocholine
d-DPPC	1,2-dipalmitoyl-*d*62-*sn*-glycero-3-phosphocholine-1,1,2,2-*d*4-*N*,*N*,*N*-trimethyl-*d*9
DPPG	1,2-dipalmitoyl-*sn*-glycero-3-[phospho-*rac*-(1-glycerol)] (sodium salt)
d-DPPG	1,2-dipalmitoyl-*d*62-*sn*-glycero-3-[phospho-*rac*-(1-glycerol)] (sodium salt)
DSPC	1,2-distearoyl-*sn*-glycero-3-phosphocholine
d-DSPC	1,2-distearoyl-*d*70-*sn*-glycero-3-phosphocholine-1,1,2,2-*d*4-*N*,*N*,*N*-trimethyl-*d*9

studies on alamethicin under membrane potential. In addition, we also investigated the lipid chain length effect on the interactions of alamethicin with model membranes using SFG.

2. Experimental Section

2.1. Materials. Alamethicin from *Trichoderma viride*, with a minimum purity of 90%, was purchased from Sigma-Aldrich (St.Louis, MO). Different lipids (listed in Table 1) were purchased from Avanti Polar Lipids (Alabaster, AL). Deuterated water (D_2O) was ordered from Aldrich (Milwaukee, WI). Right-angle CaF_2 prisms were purchased from Altos (Trabuco Canyon, CA).

All of the chemicals were used as received. CaF_2 prisms were thoroughly cleaned using a procedure with several steps: They were first soaked in toluene for 24 h and then sonicated in Contrex AP solution from Decon Laboratories (King of Prussia, PA) for 1 h. After that, they were rinsed with deionized (DI) water before soaking in methanol for 10 min. All of the prisms were then rinsed thoroughly with an ample amount of DI water and cleaned inside a glow discharge plasma chamber for 4 min immediately before depositing lipid molecules on them. Substrates were tested using SFG, and no signal from contamination was detected.

2.1.1. Preparation of Lipid Bilayers. Single lipid bilayers that can have two different leaflets were prepared on CaF_2 substrates. Langmuir−Blodgett and Langmuir−Schaefer (LB/LS) methods were used to deposit the proximal and then the distal leaflets, respectively. A KSV2000 LB system and ultrapure water from a Millipore system (Millipore, Bedford, MA) were used throughout the experiments for bilayer preparation. The detailed procedure was reported previously[65,66] and will not be repeated here.

The bilayer was immersed in water inside a 1.6-mL reservoir throughout the entire experiment, and a small amount of water could be added to the reservoir to compensate for evaporation when needed for long time scale experiments. For alamethicin−bilayer interaction experiments, ~15 μL alamethicin solution (in methanol with a concentration of 2.5 mg/mL) was injected into the reservoir. A magnetic micro stirrer was used to ensure a homogeneous concentration distribution of peptide molecules in the subphase below the bilayer.

2.2. Polarized ATR-FTIR Experiments. A Nicolet Magna-IR 550 spectrometer was used to collect attenuated total reflectance-Fourier transform infrared (ATR-FTIR) spectra with a standard 45° ZnSe ATR cell and a ZnSe grating polarizer (from Optometrics LLC). The ZnSe crystal (Specac Ltd. Woodstock, GA) was cleaned using the same procedures as the CaF_2 prisms. The lipid bilayers were prepared onto the ZnSe crystal surface using the LB/LS method mentioned above. After the lipid bilayer was deposited onto the crystal, the water that kept the bilayer hydrated was flushed multiple times with D_2O to avoid signal confusion between the O−H bending mode and the peptide amide I mode and to ensure a better S/N ratio in the peptide amide I band frequency region. After at least 2 h to allow equilibration, a background polarized spectrum of the lipid bilayer/D_2O interface was recorded. Then ~15 μL of alamethicin solution (in methanol with a concentration of 2.5 mg/mL) was injected into the above small reservoir of 1.6 mL. After at least 1 h to allow the alamethicin adsorption to reach equilibrium, a polarized spectrum was collected. Finally, the amide I signal of alamethicin on the bilayer in D_2O was obtained by subtracting the background spectrum of the bilayer/D_2O interface from the later collected spectrum after alamethicin was adsorbed and equilibrated. All the spectra collected here were averages of 256 scans with a 2 cm^{-1} resolution.

2.3. SFG. SFG is a second-order nonlinear optical spectroscopic technique that has submonolayer surface sensitivity.[44−66] Details regarding SFG theories and measurements have been extensively published[44−66] and will not be repeated here. The SFG experimental setup was similar to that described in our earlier publications and will not be presented.[65,66] In this research, all of the SFG experiments were carried out at room temperature (25 °C). SFG spectra from interfacial alamethicin with different polarization combinations including ssp (s-polarized SF output, s-polarized visible input, and p-polarized infrared input) and ppp were collected using the near total internal reflection geometry.

2.4. Orientation Determination of Peptides. ***2.4.1. Orientation Angle of Peptides Deduced from ATR-FTIR.*** ATR-FTIR spectroscopy has been widely used to analyze peptide/protein secondary structures on surfaces or at interfaces and determine the orientation of such secondary structures.[67] In ATR-FTIR studies, the tilt angle (θ) of the helices can be determined from the measured infrared linear dichroic ratio (R) in ATR-FTIR using p- and s-polarized IR beams:[67,68]

$$R = \frac{A_{\parallel}}{A_{\perp}} = \frac{E_z^2 k_z + E_x^2 k_x}{E_y^2 k_y} \tag{1}$$

where E_i ($i = x, y, z$) is the electric field amplitude of the evanescent wave at the surface of the internal reflection element, and k_i ($i = x, y, z$) is a component of the integrated absorption coefficient in the lab-fixed coordinate system. E_i ($i = x, y, z$) depends on the incidence angle of the IR beam at the solid−liquid interface, and the refractive indices of the internal reflection element (ATR crystal), the thin film (bilayer), and the bulk contacting medium (D_2O). We calculated the value of E_i ($i = x, y, z$) using the formula published in the literature.[67,68] If we model the orientation distribution of a helix in the lab-fixed coordinate system as a Gaussian distribution ($f = (1/(2\pi)^{1/2}\sigma)e^{-(x-\theta)^2/(2\sigma^2)}$, k_i ($i = x, y, z$) is given as follows:[68]

$$\langle k_x \rangle = \langle k_y \rangle = \frac{\cos(\alpha)^2\left(\frac{1}{2} - \frac{\cos(2\theta)}{2e^{2\sigma^2}}\right)}{2} + \frac{\sin(\alpha)^2}{4} + \frac{\sin(\alpha)^2\left(\frac{1}{2} + \frac{\cos(2\theta)}{2e^{2\sigma^2}}\right)}{2} \tag{2}$$

$$\langle k_z \rangle = \cos(\alpha)^2\left(\frac{1}{2} + \frac{\cos(2\theta)}{2e^{2\sigma^2}}\right) + \frac{\sin(\alpha)^2\left(\frac{1}{2} - \frac{\cos(2\theta)}{2e^{2\sigma^2}}\right)}{2} \quad (3)$$

where θ and σ are the tilt angle between the helix's principal axis and the surface normal and the orientation distribution width, respectively; α is the angle between the transition dipole moment and the principal axis of the helix, which is equal to 38° for α-helix and 45° for 3_{10}-helix.[69,70] The bracket denotes the time and ensemble average. When $\sigma = 0$, the orientation distribution is a δ-distribution. Since ATR-FTIR provides only one experimentally measured parameter (R), based on eqs 1−3, the tilt angle θ can be determined by knowing the value of E_i ($i = x, y, z$), α, and assuming a certain value of σ. Here, we used a delta distribution.

2.4.2. Orientation Angle of Peptides Deduced from SFG. The molecular orientation information can be obtained by relating SFG susceptibility tensor elements $\chi_{ijk}(i, j, k = x, y, z)$ to the SFG molecular hyperpolarizability tensor elements $\beta_{lmn}(l, m, n = a, b, c)$.[44−66] Our lab has developed a methodology to determine the orientation of α-helical structures using SFG amide I spectra collected with different polarization combinations. This method has been introduced in our previous papers[66,71−75] and will not be repeated here.

Similar to the method for an α-helix, we developed the orientation analysis method for a 3_{10}-helix in membrane.[72] We deduced the relation between the χ_{ppp}/χ_{ssp} value and the 3_{10}-helix orientation with a δ or Gaussian distribution using different hyperpolarizability tensor elements with the adoption of the bond additivity model. Thus, the orientation angle (θ) of a 3_{10}-helix can be deduced by measuring the ppp and ssp spectral intensity ratio of the peptide amide I signals.

3. Results and Discussion

3.1. Interaction between Alamethicin and *d*-DMPC/DMPC Bilayer. ***3.1.1. SFG Results.*** SFG ssp and ppp spectra of alamethicin in a *d*-DMPC/DMPC bilayer are shown in Figure 1. The spectra were collected after 15 μL of alamethicin/methanol solution was injected into the subphase (~1.6 mL)

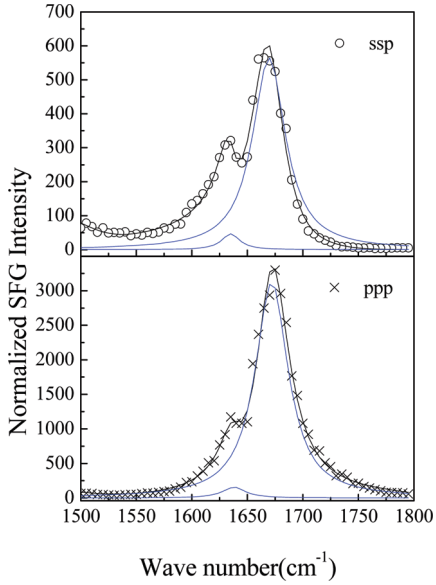

Figure 1. SFG spectra of alamethicin in a *d*-DMPC/DMPC bilayer at pH = 6.7. Top, ssp spectrum; bottom, ppp spectrum.

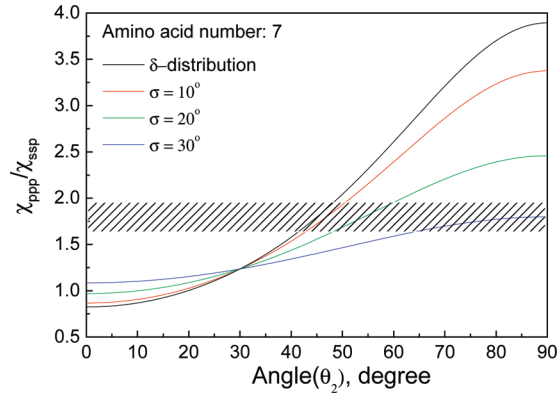

Figure 2. The relation between SFG susceptibility tensor component ratio and the 3_{10}-helix orientation angle. The measured orientation angle is about 43° (between 39° and 47°), assuming a narrow angle distribution.

of a *d*-DMPC/DMPC bilayer at pH 6.7. The SFG spectra are dominated by two peaks at 1635 and 1670 cm^{-1}, which is consistent with the results of previous FTIR and Raman studies in which the amide I peaks centered at 1639 and 1662 cm^{-1} were observed in membrane-incorporated alamethicin.[76−78] The frequency of the 1662 cm^{-1} peak in IR spectra is higher than those normally found for soluble or membrane-inserted α-helices (usually at ~1650 cm^{-1}). Chapman et al. conclude that this higher frequency is an indication for a 3_{10}-helical structure connected to the α-helix in alamethicin in lipid bilayers.[76] Therefore, we believe that the 1670 cm^{-1} peak observed in the SFG spectra is contributed by a helical structure dominated by an α-helix but with a 3_{10}-helix part. Peak assignments in the literature indicate that the 1635 cm^{-1} peak is due to the 3_{10}-helix.[76−79]

Alamethicin consists of two helical segments because of the presence of the helix-breaking Pro14 residue.[24] According to the above discussion, the 3_{10}-helix formed by residues 14−20 contributes to the signal at 1635 cm^{-1}; the α-helical/3_{10}-helical structure (mainly the α-helical component) which contains residues 1−13 contributes to the signal at 1670 cm^{-1}. Here, we define the tilt angle between the principal axis of the helix with the residues 1−13 and the *d*-DMPC/DMPC bilayer surface normal to be θ_1 and the tilt angle between the principal axis of the helix composed of residues 14−20 and the *d*-DMPC/DMPC bilayer surface normal to be θ_2.

(A) Orientation of 3_{10}-Helix Containing Residues 14−20 (θ_2). Using the relation between the measured ppp and ssp spectral intensity ratio of the peak at 1635 cm^{-1}, we should be able to determine the orientation angle (θ_2). We deduced the hyperpolarizability tensor elements for a 3_{10}-helix that consists of seven amino acid residues and obtained $\beta_{aca} = 0.54\beta_{ccc}$ and $\beta_{aac} = 1.1\beta_{ccc}$. Details regarding the deduction of specific tensor elements of 3_{10}-helix were reported previously[72] and will not be repeated here. As a result of the deduction, a relation between the measured χ_{ppp}/χ_{ssp} ratio and the 3_{10}-helix orientation for a 3_{10}-helix with seven amino acids is presented in Figure 2.[72] Here, the experimentally measured χ_{ppp}/χ_{ssp} ratio of the peak at 1635 cm^{-1} in the *d*-DMPC/DMPC bilayer is 1.80 ± 0.15; therefore, the orientation angle θ_2 is about 43° (between 39° and 47°). The number of amino acid residues in an ideal 3_{10}-helix should be multiples of 3. There are some concerns that the 3_{10}-helical symmetry may be slightly broken when the number of the amino acids in a 3_{10}-helix deviates from multiples of 3. In that case, the relation between the χ_{ppp}/χ_{ssp} value and 3_{10}-helix orientation may vary when the number of the amino acids in a 3_{10}-helix

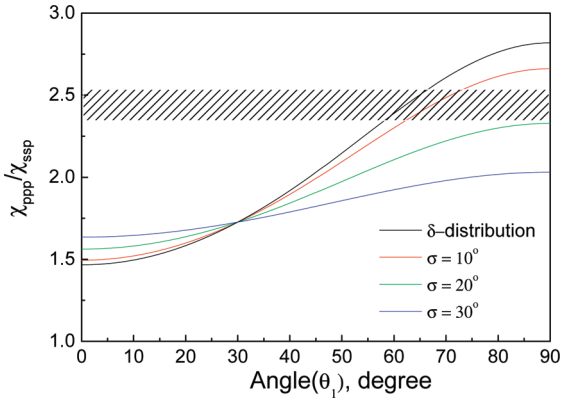

Figure 3. The relation between SFG susceptibility tensor component ratio for the helix containing 1−13 residues and the helix orientation angle. The measured orientation angle is about 63° (between 57° and 68°), assuming a narrow angle distribution.

changes. To address the above concern, we calculated β_{aac}/β_{ccc}, β_{aca}/β_{ccc} for 3_{10}-helices having three to seven amino acids.[72] Using the calculated parameters, the ratio of χ_{ppp}/χ_{ssp} as a function of 3_{10}-helix orientation angle (θ_2) can be deduced. The results indicated that the orientation determination is not noticeably affected by the numbers of amino acids in a 3_{10}-helix when the tilt angle is smaller than 50°.

(B) Orientation of the Helix Containing Residues 1−13 (θ_1). The orientation angle (θ_1) can be deduced by using the relation between the measured ppp and ssp spectral intensity ratio of the peak at 1670 cm^{-1}. We deduced the hyperpolarizability tensor elements for the helix that consists of residues 1−13, which contains both α- and 3_{10}-helical structures (mainly α-helical elements). Recently, Salnikov et al. studied the structure and alignment of uniformly ^{15}N-labeled alamethicin in POPC and DMPC membranes using oriented ^{15}N and ^{31}P solid state NMR spectroscopy.[27] A model structure with an α-helix formed by the first 10 residues and a 3_{10}-helix formed by the next 10 residues was found to be able to predict the features in the observed NMR spectrum reasonably well.[27] Here, we propose that the helix formed by residues 1−13 has two portions: an α-helix formed by the first 10 residues and a 3_{10}-helix formed by the residues 11−13. The relation between the χ_{ppp}/χ_{ssp} ratio of this structure and its membrane orientation is presented in Figure 3.

The experimentally measured χ_{ppp}/χ_{ssp} ratio for the peak at 1670 cm^{-1} in the *d*-DMPC/DMPC bilayer is about 2.45 ± 0.15, yielding an orientation angle θ_1 of about 63° (between 57° and 68°). Although this value of θ_1 is deduced from the above proposed structure with an α-helix formed by the first 10 residues and 3_{10}-helix formed by residues 11−13, θ_1 did not substantially change when different structures were used in orientation determination, as shown in Table 2.

We note that the bend angle between the two helical components in alamethicin ($\theta_1-\theta_2$) is about 20° in this study, assuming the plane containing both helical components is perpendicular to the membrane surface. This is in excellent agreement with previous results: 17° was reported in DMPC−bilayer-associated alamethicin,[26] and 20−35° in crystallized alamethicin.[24]

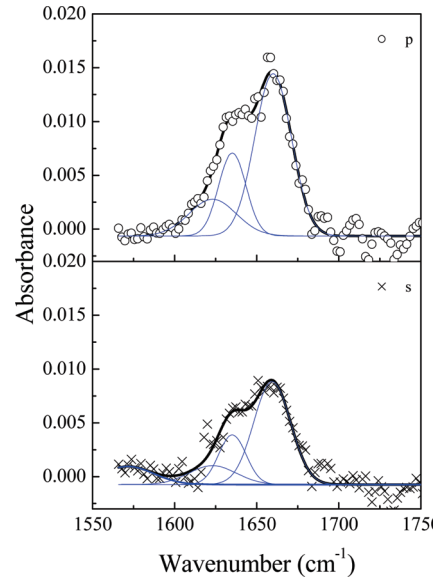

Figure 4. Polarized ATR-FTIR spectra of alamethicin in a *d*-DMPC/DMPC bilayer at pH = 6.7. Top, p-polarized spectrum; bottom, s-polarized spectrum.

TABLE 3: Interactions between Alamethicin and Different Lipid Bilayers

inner layer	outer layer	transition temperature of outer layer lipid (°C)[a]	phase of outer layer lipid at experimental condition	SFG signal
POPC	POPC	−2	fluid	very strong
POPC	POPG	−2	fluid	very strong
d-DMPC	*d*-DMPC	23	fluid	very strong
d-DMPC	DMPC	23	fluid	very strong
d-DPPC	DPPC	41	gel	weak
d-DPPG	DPPG	41	gel	weak
d-DSPC	DSPC	55	gel	weak

[a] http://www.avantilipids.com/PhaseTransitionTemperaturesForGlycerophospholipids.html.

3.1.2. ATR-FTIR Results. ATR-FTIR was used as a supplemental technique to substantiate SFG results. ATR-FTIR polarized spectra of alamethicin in a *d*-DMPC/DMPC bilayer are displayed in Figure 4. According to the previous results in the literature, we fit these spectra using three peaks centered at 1623, 1635, and 1660 cm^{-1}. The intensity ratio (R) of the signal measured using the p- versus s-polarized beam is 1.7 for the 1635 cm^{-1} peak and 1.6 for the 1660 cm^{-1} peak. From this R value, the orientation angle can be calculated to be 55° for θ_1 (between 52° and 58°) and 49° for θ_2 (between 45° and 53°), assuming a δ-orientation distribution; they are not very different from the SFG results of $\theta_1 = 63°$ and $\theta_2 = 43°$ presented above. The difference between the SFG and ATR-FTIR results might be due to the fact that the orientation distribution is not a delta distribution.

Both our SFG and ATR-FTIR studies indicated that alamethicin molecules exhibit a large tilt angle versus the surface normal in a *d*-DMPC/DMPC bilayer. These results agree with those from recent ATR-FTIR research on fluid-phase lipid-

TABLE 2: The Orientation Angle, θ_1, of Different Proposed Structures of the Helix Containing Residues 1−13 in Alamethicin

modeling structure	structure description	orientation angle (θ_1)
model 1	α-helix with 1−10 residues, 3_{10}-helix with 11−13 residues	63 (between 57 and 68°)
model 2	α-helix with 1−9 residues, 3_{10}-helix with 10−13 residues	64 (between 58 and 70°)
model 3	α-helix with 1−11 residues, 3_{10}-helix with 12−13 residues	64 (between 57 and 69°)
model 4	only α-helix with 1−10 residues	63 (between 56 and 69°)

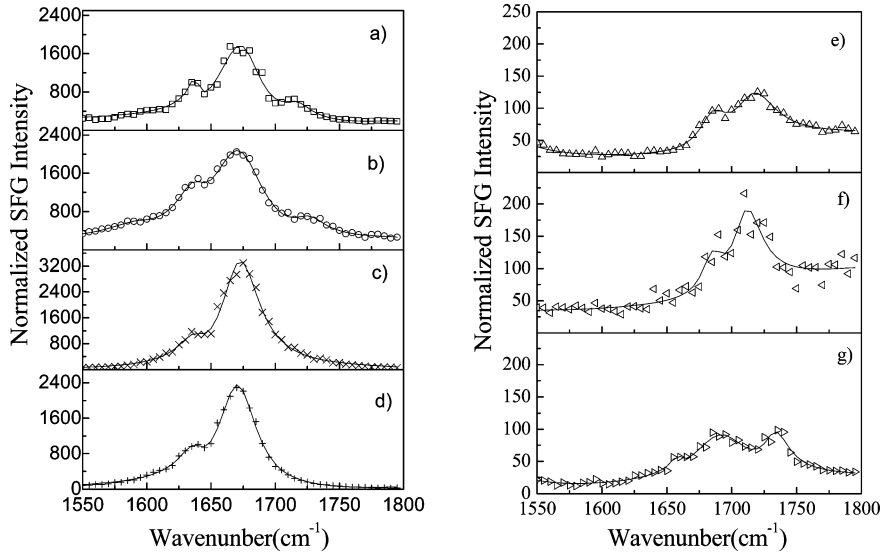

Figure 5. SFG ppp spectra of alamethicin in different bilayers at pH = 6.7: (a) POPC/POPC; (b) POPC/POPG; (c) *d*-DMPC/DMPC; (d) *d*-DMPC/*d*-DMPC; (e) *d*-DPPC/DPPC; (f) *d*-DPPG/DPPG; and (g) *d*-DSPC/DSPC.

membrane-associated alamethicin.[32,36] Marsh reported that the tilt angle of alamethicin is 67° in 1,2-didecanoyl-*sn*-glycero-3-phosphocholine membranes, and 51° in 1,2-diundecanoyl-*sn*-glycero-3-phosphocholine membranes at 36 °C.[36] In addition, Stella et al. observed that the tilt angle of alamethicin is about 60° in a POPC bilayer membrane.[32]

In contrast, our results are quite different from those obtained from labeled alamethicin in NMR or electron paramagnetic resonance (EPR) studies. Site-specific ^{15}N-labeled alamethicin was found to be more or less parallel to the DMPC bilayer normal[25] or slightly tilted (10−20°) determined by solid-state ^{15}N NMR.[26] In addition, it was shown by solid-state ^{15}N and ^{31}P NMR spectroscopy that uniformly ^{15}N-labeled alamethicin orients parallel to the POPC and DMPC membrane surface normal.[27] EPR studies indicated that TOAC-substituted alamethicin orients with a tilt angle varying from 23° to 13° in a fluid-phase diacyl phosphatidylcholine bilayer at 75 °C.[35] It has been suggested that the measured orientation of alamethicin on membranes depends on the experimental conditions.[41,42] We also agree that the different methods may lead to varying results. NMR studies require complicated sample preparation procedures as well as exogenous labels. The effective order parameters measured by EPR with TOAC-substituted alamethicin are relative to the local membrane director.[35] This local tilt of transmembrane polypeptides has been augmented by thermally excited elastic bending fluctuations of the entire membrane.[80,81] These fluctuations can change the elastic modulus for membrane area expansion,[82] facilitating the insertion of transmembrane proteins/peptides, and also can give rise to a net inclination of the local membrane normal (or director), to which the molecular tilt of the peptide is referred.[82]

3.2. Interaction between Alamethicin and Different Lipid Bilayers. It has been shown that the membrane lipid chain length affects the interactions between alamethicin and cell membranes.[21,34−36,83,84] Recently, Marsh et al. investigated the dependence of the incorporation of spin-labeled alamethicin into fluid phosphatidylcholine membrane bilayers on a lipid chain length using EPR. Their results suggested that the orientation and aggregation of alamethicin are related to the chain length of the lipid. The lipid chain length can modulate the activity of transmembrane proteins/peptides by the mismatch between the hydrophobic span of the protein/peptide and the lipid membrane.[34−36] In this study, we observed markedly different SFG signal intensities from alamethicin in bilayers with lipids of different chain lengths. The different lipids examined and varied SFG results are listed in Table 3. It is well-known that the lipid chain length is one of the factors that determine the phase of the lipid bilayer at room temperature: Similar lipids with longer chains tend to exist in the gel phase, whereas shorter chains are likely in the fluid phase.

Figure 5 shows the ppp SFG spectra collected after 15 μL of alamethicin/methanol solution was injected into the subphase (~1.6 mL) of various bilayers. In the fluid-phase lipid bilayers (Figure 5a−d), strong SFG amide I signals of alamethicin were observed, dominated by two peaks at 1635 and 1670 cm^{-1}. These two peaks are contributed by the 3_{10}-helical structure and the α-helical structure of alamethicin. Using the orientation analysis method discussed above, the orientations of alamethicin in different lipids were investigated. The deduced results indicated that the orientations of alamethicin in different fluid-phase lipid bilayers (POPC/POPC, POPC/POPG, d-DMPC/d-DMPC bilayers) are similar to each other and, thus, also similar to the one presented above regarding the *d*-DMPC/DMPC bilayer. Therefore, it is concluded that alamethicin has a highly ordered orientation in fluid-phase lipid bilayers with a large tilt angle.

When alamethicin was interacting with gel-phase lipid bilayers (Figure 5e−g), only two weak SFG peaks at 1685 and 1720 cm^{-1} were observed. We believe that the peak at 1685 cm^{-1} is contributed by the antiparallel β-sheet or aggregated strand of peptides.[61,67] The 1720 cm^{-1} signal is not the amide I signal from alamethicin; instead, it originates from the carbonyl groups of the lipid bilayer. The absence of the strong alamethicin helical signal on the gel-phase lipid bilayer indicates that both the helical structures lie down on the lipid bilayer surface or may be changed into other secondary structures; for example, an antiparallel β-sheet or aggregated strand. This is consistent with the results obtained using other analytical tools in the literature.[38−40] Therefore, it is evident that alamethicin interacts with gel-phase and fluid-phase lipid bilayers differently.

4. Conclusion

We applied SFG to investigate the molecular interactions between alamethicin, an important model for larger channel

proteins, and different lipid bilayers in situ and in real time without exogenous labeling. It was found that alamethicin interacts differently with gel-phase versus fluid-phase lipid bilayers. When alamethicin molecules interact with gel-phase lipid bilayers, they lie down, aggregate on the gel-phase bilayer surface, or both. We believe that they do not have significant insertion into the lipid bilayers. Differently, alamethicin molecules can insert into fluid-phase lipid bilayers with large tilt angels in the absence of membrane potential. The orientation of alamethicin in fluid-phase lipid bilayers was determined by deducing the orientations of the α- and 3_{10}- helical structural segments using polarized SFG amide I spectra and substantiated by the polarized ATR-FTIR studies. To our knowledge, this is the first time that SFG has been successfully applied to determine the orientation of a 3_{10}-helix experimentally. The formation of channels by alamethicin under membrane potential will be investigated in the future to elucidate molecular mechanisms of these channels.

Acknowledgment. This research is supported by National Institute of Health (1R01GM081655-01A2) and Office of Naval Research (N00014-02-1-0832 and N00014-08-1-1211). S.Y. acknowledges start-up funding from the University of Science and Technology of China and Chinese Universities Scientific Fund.

References and Notes

(1) Kelkar, D. A.; Chattopadhyay, A. *Biochim. Biophys. Acta* **2007**, *1768*, 2011–2025.
(2) Cooper, E. C.; Jan, L. Y. *Proc. Natl. Acad. Sci. U.S.A.* **1999**, *96*, 4759–4766.
(3) Jentsch, T. J.; Hübner, C. A.; Fuhrmann, J. C. *Nat. Cell Biol.* **2004**, *6*, 1039–1047.
(4) Verkman, A. S.; Galietta, L. J. V. *Nat. Rev. Drug Discov.* **2009**, *8*, 153–171.
(5) Berger, A. L.; Ikuma, M.; Welsh, M. J. *Proc. Natl. Acad. Sci. U.S.A.* **2005**, *102*, 455–460.
(6) Gadsby, D. C.; Vergani, P.; Csanady, L. *Nature* **2006**, *440*, 477–483.
(7) Tan, H. L.; Bink-Boelkens, M. T. E.; Bezzina, C. R.; Viswanathan, P. C.; Beaufort-Krol, G. C. M.; van Tintelen, P. J.; van den Berg, M. P.; Wilde, A. A. M.; Balser, J. R. *Nature* **2001**, *409*, 1043–1047.
(8) Armstrong, N.; Sun, Y.; Chen, G. Q.; Gouaux, E. *Nature* **1998**, *395*, 913–917.
(9) Stutts, M. J.; Canessa, C. M.; Olsen, J. C.; Hamrick, M.; Cohn, J. A.; Rossier, B. C.; Boucher, R. C. *Science* **1995**, *269*, 847–850.
(10) Sansom, M. S. P. *Prog. Biophys. Mol. Biol.* **1991**, *55*, 139–235.
(11) Woolley, G. A.; Wallace, B. A. *J. Membr. Biol.* **1992**, *129*, 109–136.
(12) Sansom, M. S. P. *Eur. Biophys. J.* **1993**, *22*, 105–124.
(13) Sansom, M. S. P. *Q. Rev. Biophys.* **1993**, *26*, 365–421.
(14) Cafiso, D. S. *Annu. Rev. Biophys. Biomol. Struct.* **1994**, *23*, 141–165.
(15) Marsh, D. *Biochem. J.* **1994**, *23*, 345–361.
(16) Bechinger, B. *J. Membr. Biol.* **1997**, *156*, 197–211.
(17) Duclohier, H.; Wroblewski, H. *J. Membr. Biol.* **2001**, *184*, 1–12.
(18) Nagaraj, R.; Balaram, P. *Acc. Chem. Res.* **1981**, *14*, 356–362.
(19) Kessel, A.; Cafiso, D. S.; Ben-Tal, N. *Biophys. J.* **2000**, *78*, 571–583.
(20) Mathew, M. K.; Balaram, P. *Mol. Cell. Biochem.* **1983**, *50*, 47–64.
(21) Hall, J. E.; Vodyanoy, I.; Balasubramanian, T. M.; Marshall, G. R. *Biophys. J.* **1984**, *45*, 233–247.
(22) Mathew, M. K.; Balaram, P. *FEBS Lett.* **1983**, *157*, 1–5.
(23) Leitgeb, B.; Szekeres, A.; Manczinger, L.; Vagvolgyi, C.; Kredics, L. *Chem. Biodiversity* **2007**, *4*, 1027–1051.
(24) Fox, R. O.; Richards, F. M. *Nature* **1982**, *300*, 325–330.
(25) North, C. L.; Barranger-Mathys, M.; Cafiso, D. S. *Biophys. J.* **1995**, *69*, 2392–2397.
(26) Bak, M.; Baywater, R. P.; Hohwy, M.; Thomsen, J. K.; Adelhorst, K.; Jakobsen, H. J.; Sorensen, O. W.; Nielsen, N. C. *Biophys. J.* **2001**, *81*, 1684–1698.
(27) Salnikov, E. S.; Friedrich, H.; Li, X.; Bertani, P.; Reissmann, S.; Hertweck, C.; O'Neil, J. D. J.; Raap, J.; Bechinger, B. *Biophys. J.* **2009**, *96*, 86–100.
(28) Duclohier, H. *Eur. Biophys. J.* **2004**, *33*, 169–174.
(29) Laver, D. R. *Biophys. J.* **1994**, *66*, 355–359.
(30) Vodyanoy, I.; Hall, J. E.; Balasubramanian, T. M. *Biophys. J.* **1983**, *42*, 71–82.
(31) Milov, A. D.; Samoilova, R. I.; Tsvetkov, Y. D.; Zotti, M. D.; Toniolo, C.; Raap, J. *J. Phys. Chem. B* **2008**, *112*, 13469–13472.
(32) Stella, L.; Burattini, M.; Mazzuca, C.; Palleschi, A.; Venanzi, M.; Coin, I.; Peggion, C.; Toniolo, C.; Pispisa, B. *Chem. Biodiversity* **2007**, *4*, 1299–1312.
(33) Kessel, A.; Cafiso, D. S.; Ben-Tal, N. *Biophys. J.* **2000**, *78*, 571–583.
(34) Marsh, D.; Jost, M.; Peggion, C.; Toniolo, C. *Biophys. J.* **2007**, *92*, 473–481.
(35) Marsh, D.; Jost, M.; Peggion, C.; Toniolo, C. *Biophys. J.* **2007**, *92*, 4002–4011.
(36) Marsh, D. *Biochemistry* **2009**, *48*, 729–737.
(37) Salnikov, E. S.; Zotti, M. D.; Formaggio, F.; Li, X.; Toniolo, C.; O'Neil, J. D. J.; Raap, J.; Dzuba, S. A.; Bechinger, B. *J. Phys. Chem. B* **2009**, *113*, 3034–3042.
(38) Banerjee, U.; Zidovetzki, R.; Birge, R. R.; Chan, S. I. *Biochemistry* **1985**, *24*, 7621–7627.
(39) Ionov, R.; El-Abed, A.; Angelova, A.; Goldmann, M.; Peretti, P. *Biophys. J.* **2000**, *78*, 3026–3035.
(40) Mottamal, M.; Lazaridis, T. *Biophys. Chem.* **2006**, *122*, 50–57.
(41) Chen, F. Y.; Lee, M. T.; Huang, H. W. *Biophys. J.* **2002**, *82*, 908–914.
(42) Huang, H. W.; Wu, Y. *Biophys. J.* **1991**, *60*, 1079–1087.
(43) Spaar, A.; Munster, C.; Salditt, T. *Biophys. J.* **2004**, *87*, 396–407.
(44) Miranda, P. B.; Shen, Y. R. *J. Phys. Chem. B* **1999**, *103*, 3292–3307.
(45) Kim, J.; Somorjai, G. A. *J. Am. Chem. Soc.* **2003**, *125*, 3150–3158.
(46) Kim, J.; Cremer, P. S. *ChemPhysChem.* **2001**, *2*, 543–546.
(47) Li, G.; Ye, S.; Morita, S.; Nishida, T.; Osawa, M. *J. Am. Chem. Soc.* **2004**, *126*, 12198–12199.
(48) Voges, A. B.; Al-Abadleh, H. A.; Musorrariti, M. J.; Bertin, P. A.; Nguyen, S. T.; Geiger, F. M. *J. Phys. Chem. B* **2004**, *108*, 18675–18682.
(49) Li, Q. F.; Hua, R.; Chea, I. J.; Chou, K. C. *J. Phys. Chem. B* **2008**, *112*, 694–697.
(50) Ye, H. K.; Gu, Z. Y.; Gracias, D. H. *Langmuir* **2006**, *22*, 1863–1868.
(51) Yatawara, A. K.; Tiruchinapally, G.; Bordenyuk, A. N.; Andreana, P. R.; Benderskii, A. V. *Langmuir* **2009**, *25*, 1901–1904.
(52) Perry, A.; Ahlborn, H.; Space, B.; Moore, P. B. *J. Chem. Phys.* **2003**, *118*, 8411–8419.
(53) Liu, J.; Conboy, J. C. *Biophys. J.* **2005**, *89*, 2522–2532.
(54) Chen, X.; Wang, J.; Sniadecki, J. J.; Even, M. A.; Chen, Z. *Langmuir* **2005**, *21*, 2662–2664.
(55) Ye, S. J.; McClelland, A.; Majumdar, P.; Stafslien, S.; Daniels, J.; Chisholm, B.; Chen, Z. *Langmuir* **2008**, *24*, 9686–9694.
(56) Wang, J.; Paszti, Z.; Clarke, M. L.; Chen, X.; Chen, Z. *J. Phys. Chem. B* **2007**, *111*, 6088–6095.
(57) Chen, X.; Wang, J.; Paszti, Z.; Wang, F.; Schrauben, J. N.; Tarabara, V. V.; Schmaier, A. H.; Chen, Z. *Anal. Bioanal. Chem.* **2007**, *388*, 65–72.
(58) Wang, J.; Chen, X.; Clarke, M. L.; Chen, Z. *J. Phys. Chem. B* **2006**, *110*, 5017–5024.
(59) Clarke, M. L.; Wang, J.; Chen, Z. *J. Phys. Chem. B* **2005**, *109*, 22027–22035.
(60) Wang, J.; Clarke, M. L.; Chen, X.; Even, M. A.; Johnson, W. C.; Chen, Z. *Surf. Sci.* **2005**, *587*, 1–11.
(61) Ye, S. J.; Nguyen, K. T.; Le Clair, S.; Chen, Z. *J. Struct. Biol.* **2009**, *168*, 61–77.
(62) Chen, X.; Chen, Z. *Biochim. Biophys. Acta* **2006**, *1758*, 1257–1273.
(63) Chen, X.; Clarke, M. L.; Wang, J.; Chen., Z. *Int. J. Mod. Phys. B* **2005**, *19*, 691–713.
(64) Ye, S. J.; Nguyen, K. T.; Boughton, A. P.; Mello, C. M.; Chen, Z. *Langmuir* 2010. in press (http://pubs.acs.org/doi/pdf/10.1021/la903932w).
(65) Chen, X.; Wang, J.; Kristalyn, C. B.; Chen., Z. *Biophys. J.* **2007**, *93*, 866–875.
(66) Chen, X.; Wang, J.; Boughton, A. P.; Kristalyn, C. B.; Chen, Z. *J. Am. Chem. Soc.* **2007**, *129*, 1420–1427.
(67) Tamm, L. K.; Tatulian, U. A. *Q. Rev. Biophys.* **1997**, *30*, 365–429.
(68) Kass, I.; Arbey, E.; Arkin, I. T. *Biophys. J.* **2004**, *86*, 2502–2507.
(69) Marsh, D.; Muller, M.; Schmitt, F.-J. *Biophys. J.* **2000**, *78*, 2499–2510.
(70) Malcolm, B. R.; Walkinshaw, M. D. *Biopolymers* **1986**, *25*, 607–625.
(71) Wang, J.; Lee, S. H.; Chen, Z. *J. Phys. Chem. B* **2008**, *112*, 2281–2290.
(72) Nguyen, K. T.; Le Clair, S.; Ye, S. J.; Chen, Z. *J. Phys. Chem. B* **2009**, *113*, 12169–12180.

(73) Nguyen, K. T.; Le Clair, S.; Ye, S. J.; Chen, Z. *J. Phys. Chem. B* **2009**, *113*, 12358–12363.
(74) Lee, S.; Wang, J.; Krimm, S.; Chen, Z. *J. Phys. Chem. A* **2006**, *110*, 7035–7044.
(75) Chen, X.; Boughton, A. P.; Tesmer, J. J. G.; Chen, Z. *J. Am. Chem. Soc.* **2007**, *129*, 12658–12659.
(76) Haris, P. I.; Chapman, D. *Biochim. Biophys. Acta* **1988**, *943*, 375–380.
(77) Haris, P. I.; Molle, G.; Duclohier, H. *Biophys. J.* **2004**, *86*, 248–253.
(78) Vogel, H. *Biochemistry* **1987**, *26*, 4562–4572.
(79) Kennedy, D. F.; Crisma, M.; Toniolo, C.; Chapman, D. *Biochemistry* **1991**, *30*, 6541–6548.
(80) Marsh, D. *Biophys. J.* **2008**, *94*, 3996–4013.
(81) Marsh, D.; Shanmugavadivu, B.; Kleinschmidt, J. H. *Biophys. J.* **2006**, *91*, 227–232.
(82) Marsh, D. *Biophys. J.* **1997**, *73*, 865–869.
(83) Archer, S. J.; Ellena, J. F.; Cafiso, D. S. *Biophys. J.* **1991**, *60*, 389–398.
(84) Barranger-Mathys, M.; Cafiso, D. S. *Biophys. J.* **1994**, *67*, 172–176.

JP911174D